




# Artificial neural network for aspect ratio prediction of lignocellulosic micro/nanofibers

Alexandre F. Santos · Roberto Aguado · Marcos L. Corazza · Quim Tarrés · Jose-Luis Sanchez-Salvador · Angeles Blanco · Carlos Negro · Marc Delgado-Aguilar 

Received: 21 February 2022 / Accepted: 28 April 2022 / Published online: 24 May 2022  
© The Author(s) 2022

**Abstract** In this work a wide sample analysis, under similar conditions, has been carried out and a calibration strategy based on a careful selection of input variables combined with sensitivity analysis has enabled us to build accurate neural network models, with high correlation ( $R > 0.99$ ), for the prediction of the aspect ratio of micro/nanofiber products. The model is based on cellulose content, applied energy, fiber length and diameter of the pre-treated pulps. The number of samples used to generate the neural network model was relatively low, consisting of just 15 samples coming from pine pulps that had undergone thermomechanical, kraft and bleached kraft treatments to produce a significant range of aspect ratio.

However, the ANN model, involving 4 inputs and 4 hidden neurons and calibrated on the basis of pine dataset, was accurate and robust enough to predict the aspect ratio of micro/nanofiber materials obtained from other cellulose sources including very different softwood and hardwood species such as Spruce, Eucalyptus and Aspen ( $R = 0.84$ ). The neural network model was able to capture the nonlinearities involved in the data providing insight about the profile of the aspect ratio achieved with further homogenization during the fibrillation process.

**Keywords** Lignocellulosic micro/nanofibers · Machine learning · Artificial neural networks

**Supplementary Information** The online version contains supplementary material available at <https://doi.org/10.1007/s10570-022-04631-5>.

A. F. Santos · R. Aguado · Q. Tarrés · M. Delgado-Aguilar (✉)  
LEPAMAP-PRODIS Research Group, University of Girona, C/ Maria Aurèlia Capmany, 61, 17003 Girona, Spain  
e-mail: m.delgado@udg.edu

A. F. Santos · M. L. Corazza  
Department of Chemical Engineering, Federal University of Paraná, Curitiba, PR CEP 81531-990, Brazil

J.-L. Sanchez-Salvador · A. Blanco · C. Negro  
Department of Chemical Engineering and Materials, University Complutense of Madrid, Avda. Complutense s/n, 28040 Madrid, Spain

## Introduction

Nanostructured cellulose, broadly known as nanocellulose (NC), has attracted much interest from the scientific and technological community due to its outstanding properties, bio-based origin, biocompatibility, capacity to be easily functionalized, and biodegradability (Klemm et al. 2018). Taking advantage of the hierarchical structure of lignocellulosic fibers, NC is usually produced by means of top-down approaches, this is deconstructing the cell wall into nanosized cellulosic materials, which may exhibit different morphology, composition and structural attributes depending on the raw material, production strategy and treatment intensity (Li et al. 2021b). The

literature reports two main top-down structures: cellulose nanofibers (CNFs) and cellulose nanocrystals (CNCs), which differ in terms of production methods, morphology, structure, and properties (Kim et al. 2015). On the one hand, CNFs consist of fibrils with nanosized diameters with a high aspect ratio, above 50, high surface area, ranging from 100 to 350 m<sup>2</sup>/g, and great ability to form strong, flexible, and dimensionally stable 3D-structured networks due to the presence of both amorphous and crystalline regions (Tarrés et al. 2017a). Further, depending on the fibrillation degree, they might be referred to as cellulose microfibrils (CMFs) or microfibrillated cellulose (MFC). In addition, when the starting material contains lignin, some authors referred to this class of CNFs as lignocellulosic nanofibers (LCNFs) or lignocellulosic micro/nanofibers (LCMNFs) (Ferrer et al. 2012; Tarrés et al. 2017b; Serra-Parareda et al. 2021c). On the other hand, the CNC production process consists of acid hydrolysis, which dissolves most of the amorphous fraction and results in rod-like structures in the nano domain. These different structural characteristics confer CNFs and CNCs great opportunities in many productive sectors, such as papermaking, biocomposites, filtration, biomedicine, or electronics, to name a few (Boufi et al. 2016; Klemm et al. 2018; Isogai 2020). Indeed, according to a recent report published by MarketsandMarkets™ in 2020, the NC market is expected to grow from USD 297 million in 2020 to USD 783 million by 2025, at a compounded annual growth rate (CAGR) of 21.3%, including both high-volume and high-added value applications (Future Markets Inc. 2020). However, these market expectations will be solely accomplished if industrial production of NC is successfully implemented and, today, there are still some limiting factors hindering this industrial deployment (Foster et al. 2018; Balea et al. 2021a).

The industrial deployment of NC production and, more concretely, CNF production, is limited by several factors, such as the huge variety of starting materials, the different production methods, and the intensity of pretreatments and fibrillation, among others (Serra-Parareda et al. 2021b). For instance, CNFs can be produced from wood, annual plants, agricultural residues (i.e. straw), recovered paper, or even the cellulosic fractions of sewage sludge from papermaking activities have been reported as potential starting material (Osong et al. 2013; Espinosa

et al. 2016; Tarrés et al. 2017a; Filipova et al. 2020; Kumar et al. 2020). This, together with the variety of chemical, enzymatic and mechanical processes and the multiple equipment available for fibrillation (i.e. high-pressure homogenizers, grinders, or microfluidizers) make the correlation between raw material characteristics, treatment nature and intensity, fibrillation method, and CNF properties a challenging task, usually unconceivable with conventional computational methods (Henriksson et al. 2007; Saito et al. 2007; Solala et al. 2012; Taheri and Samyn 2016; Gu et al. 2018; Filipova et al. 2020; Serra-Parareda et al. 2021b).

The selection of appropriate characterization methods for CNFs is becoming a topic of great interest. In a previous work, the challenges on NC characterization were identified and highlighted, which showed the need of developing real-time monitoring strategies and robust correlations between easy-to-measure variables and morphological features of CNFs (Balea et al. 2021a). In this line, Desmaisons et al. (2017) proposed a multi-criteria method to quantify the quality of CNFs, leading to a quality index. They already identified that there are several variables influencing the resulting properties and characteristics of CNFs and proposed the method for benchmarking purposes of different NC products. This represented a great advance on the state of the art, although the method reported is time consuming and requires excessive processing of the sample, which may lead to error during sample preparation (i.e. nanopaper production) (Tarrés et al. 2019).

The importance of nanostructured cellulose for several applications encourages the development of a model able to link a set of easy-to-measure operation variables and initial fiber characteristics to the morphological features of mechanically obtained CMNFs and LCMNFs. A reliable mathematical model in this case may contribute to improve the process monitoring ability, making possible the introduction of control schemes. Concerning LCMNF and CMNF production processes, even when considering all possible treatment technologies, the literature lacks accurate models. Because the rheological behaviors of suspensions are often dominated by the suspended particle's shape and size (Kangas et al. 2014), useful mathematical models based on rheological measurements have been developed to predict morphological features of CNCs and CNFs (Iwamoto et al. 2014; Tanaka et al.

2014; Wu et al. 2014, 2017; Serra-Parareda et al. 2021d). In general, these models are an adaptation of the well-known relationship between the intrinsic viscosity of suspensions and the dynamics of rod shape molecule or colloidal particles in dilute region, which is ultimately dependent on the aspect ratio (or the average length) of rigid rod-like particles (Hubbe et al. 2017; Li et al. 2021a). Although interesting nanofibril information can be found through this rheological strategy, it has been recognized that this approach loses accuracy when dealing with materials involving a wide range of aspect ratios (Iwamoto et al. 2014) and/or surface charges (Wu et al. 2017, 2019). On the one hand, those long fibers would be considered as semi-flexible rods rather than rigid rods, making the modeling approach no longer valid. On the other hand, the surface charge density of CNFs influences the electroviscous effect in the cellulose suspensions, playing a role on the viscosity measurements (Dimic-Misic et al. 2018).

The complexity of the relationships between the cellulose fibers morphology and the rest of the properties encouraged the use of several modeling approaches. Artificial neural networks (ANNs) are considered an attractive tool when working with complicated processes for which consolidated phenomenological equations are not available. This mathematical modeling approach is based on the ability of the human brain to learn from the experience, which means that the mathematical model may be “trained” with a series of patterns to predict variables of interest (Himmelblau 2000). The ANN model may improve its capacity to establish predictions when subjected to a relatively large sample data set. This technique has been applied for many years in several processes and nowadays has experienced a great boost with the popularization of machine learning algorithms and intelligent systems, which have been used for efficient handling of massive and complex data sets. Recently, the use of neural networks in the frame of the machine learning tools applied to the cellulose composites segment was reviewed, showing interesting applications related to different systems including the paper production (Torrents-Barrena and Pellicer 2021). In a related effort, Almonti et al. explored the use of ANNs to the prediction of the length of fibers of samples obtained from a cellulose refining process involving four conical refiners for paper production (Almonti et al. 2019). The input variables of these

ANN models included fiber contents, fillers amount, net refining power, pulp flow rate, refiner geometry, wear rate (considered as the hours of operation) and the mean length of incoming fibers. The final ANN model obtained after the application of statistical techniques for input variable reduction was in good agreement with the experimental data ( $R^2=0.98$ ). However, to the best of our knowledge, this tool has not yet been used to model the aspect ratio of LCMNFs, which would surely contribute to diminish uncertainty during the production processes of NC products.

For all the above, in this work, authors propose an ANN model to estimate the aspect ratio of CMNFs and LCMNFs as a function of the variables that can be characterized during the process and/or fiber characteristics that are usually provided by the supplier. The present work proposes this ANN using results available in the literature, as well as some other properties and characteristics that have been determined for this work. The sensitivity of the aspect ratio predictions to a set of inputs was verified, to retain the ANN model with high generalization ability. Additionally, ANN model validation tests were performed to infer the accuracy of the model when subjected to new materials. Overall, the present work significantly contributes to the development of industrially feasible processes for CMNF and LCMNF production, being the first work in the literature dealing with the use of ANNs in this field.

## Experimental

### Experimental data set

ANN models were constructed based on experimental data previously published by our group (Balea et al. 2021b; Sanchez-Salvador et al. 2021a; Serra-Parareda et al. 2021b). In short, 20 types of LCMNFs and CMNFs were produced combining mechanical refining and high-pressure homogenization (HPH) from different raw materials, namely (1) spruce (*Picea abies*), (2) pine (*Pinus radiata*), (3) eucalyptus (*Eucalyptus globulus*) and (4) aspen. Pine pulps had undergone thermomechanical, kraft and bleached kraft treatments (TMP, UKSP and BKSP), while the spruce pulp was a bleached thermomechanical pulp (BTMP), but all of them are softwood. In the case of

**Table 1** Previously published studies by the authors of the selected pulps and purpose in ANN model development

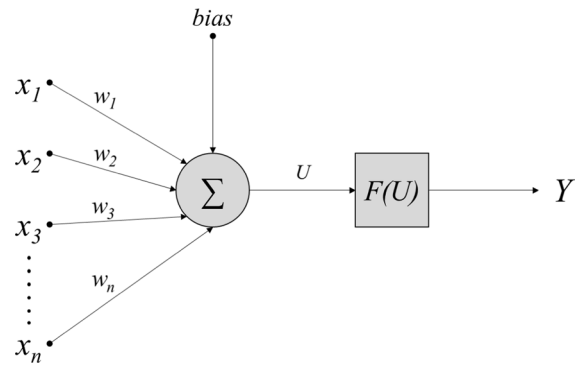
Pulp	Purpose	Reference
Pine TMP	Modelling	Serra-Parareda et al. (2021b)
Pine UKSP	Modelling	Serra-Parareda et al. (2021b)
Pine BKSP	Modelling	Serra-Parareda et al. (2021b)
Spruce BTMP	Validation	Serra-Parareda et al. (2021b)
Eucalyptus BKHP	Validation	Sanchez-Salvador et al. (2021a)
Aspen TMP	Validation	Balea et al. (2021b)

aspen pulp, it consisted of a thermomechanical pulp counting on two sulfur and chlorine free bleaching stages (Heinzel group). Finally, the eucalyptus pulp consisted of a bleached kraft pulp, kindly provided by Ence Celulosas y Energía, S.A. (Spain). All pulps have been previously used by authors in previous studies, as reported in Table 1. As it will be later discussed, pulps from pine were used for ANN modelling, while spruce, eucalyptus and aspen pulps were used for validation purposes.

The pulps were subjected to mechanical refining and HPH, gradually increasing the number of passes from 3 to 9 and pressure from 300 to 900 bar. This resulted in five HPH levels, ranging from 5.67 to 19.72 kWh/kg. Details on the pulps used for the LCMNF production are provided as supplementary material, in Table S1, while the characteristics of the obtained LCMNFs as function of the HPH intensity are provided in Table S2.

### Artificial neural network modeling

An ANN is a structure formed by simple processor elements, called neurons, interconnected through unidirectional unions associated with weights according to the chosen architecture. A typical neuron is shown in Fig. 1. The neuron has  $n$  inputs,  $x_1, x_2, \dots, x_n$ . These inputs can come from other units or from some external source, being multiplied by weights ( $w_i$ ). When introduced into the neuron, they are summed up and a constant sign ( $b$ , bias) is added to the weighted sum. The resulting signal ( $U$ ) is transformed by typically non-linear functions, called activation functions, generating the output ( $Y$ ). ANN models can assume many different configurations. In the simplest case, usually called as the feed-forward

**Fig. 1** Typical neuron receiving  $n$  inputs and a bias to produce an output signal ( $Y$ )

ANN structure, three different layers are employed: the input layer, the hidden layer, and the output layer. The input layer is fed by values of several input variables. The output layer provides the desired process response. The backpropagation procedure is normally used to estimate the ANN model parameters during the so-called model training or calibration step.

Feedforward ANN were trained using Levenberg–Marquardt backpropagation algorithm. All the feedforward networks were designed with only one hidden layer. The activation functions adopted were hyperbolic tangent and linear to hidden and output layer, respectively. According to Haykin, the hyperbolic tangent promotes a faster network learning because it is an anti-symmetric activation function (Kubat 1999). The weights and biases were initialized following the Nguyen-Widrow initialization algorithm (Nguyen and Widrow 1990).

The selection criterion of the input data for ANN modelling was based in a two-fold approach. First, out of the available data, those variables involving time-consuming methodologies were not considered and only those characteristics able to be measured rapidly and/or in real-time were considered for modelling. This first selection resulted in a set of variables, which is reported in Tables S1 and S2, that was used for determining the relative strength (RS) of each variable, as well as the optimal ANN architecture based on the lowest MSE and the highest R. In this sense, both water retention value (WRV) and yield of nanofibrillation were discarded. WRV provides a good indication of the fibrillation degree of lignocellulosic materials, both at micro and nanoscale. Indeed, it has been already proposed as monitoring

parameter of the fibrillation degree of nanostructured cellulose (Gu et al. 2018). However, in a recent study, the correlation between specific surface area (SSA) and WRV was found to not follow a linear relationship in lignin-containing micro/nanostructured cellulose, which indicates that WRV may be influenced by additional effects to morphological changes (Serra-Parareda et al. 2021c). The HPH process contributes to the release of lignin, influencing the surface chemical composition and, thus, modifying the hydrophilicity of the LCMNFs as they are passed through an HPH. This has been already reported by other authors and limits the use of this parameter for monitoring the fibrillation degree, as chemical composition should be continuously monitored as well (Qua et al. 2011; Jonooobi et al. 2015). In addition, the determination of WRV is time consuming, as it requires drying stages to quantify the amount of retained water (Gu et al. 2018). Regarding the yield of nanofibrillation, it was excluded from the input data set due to the required time to determine the amount of nanosized fraction, as it requires a centrifugation stage followed by drying of the sediment until constant weight (Tarrés et al. 2017a; Sanchez-Salvador et al. 2022).

Regarding the output variable, the aspect ratio was selected due to its significance for a wide range of applications and, in addition, for its relationship between other characteristics of CMNFs and LCMNF suspensions. As an example, the aspect ratio directly influences the reinforcing potential of LCMNFs when incorporated into paper and polymer matrices, the rheological behavior of LCMNF suspensions and their network forming capacity, particularly in porous materials such as aerogels (Tanaka et al. 2015; Boufi et al. 2016; Oksman et al. 2016; De France et al. 2017; Sanchez-Salvador et al. 2020; Serra-Parareda et al. 2021d).

All possible combinations of inputs were used to generate different networks to predict the aspect ratio of the micro/nanomaterial products and the one that provided the best response to test data was selected. The same strategy was adopted to define the number of neurons in the hidden layer. Figure 2 illustrates the architecture of a typical feedforward ANN trained in the current work.

Table 2 summarizes the variables and range values investigated for ANN modelling, which only included data from Pine TMP, Pine UKSP and Pine BKSP.

**Fig. 2** Feedforward ANN structure for a multiple input and single output problems

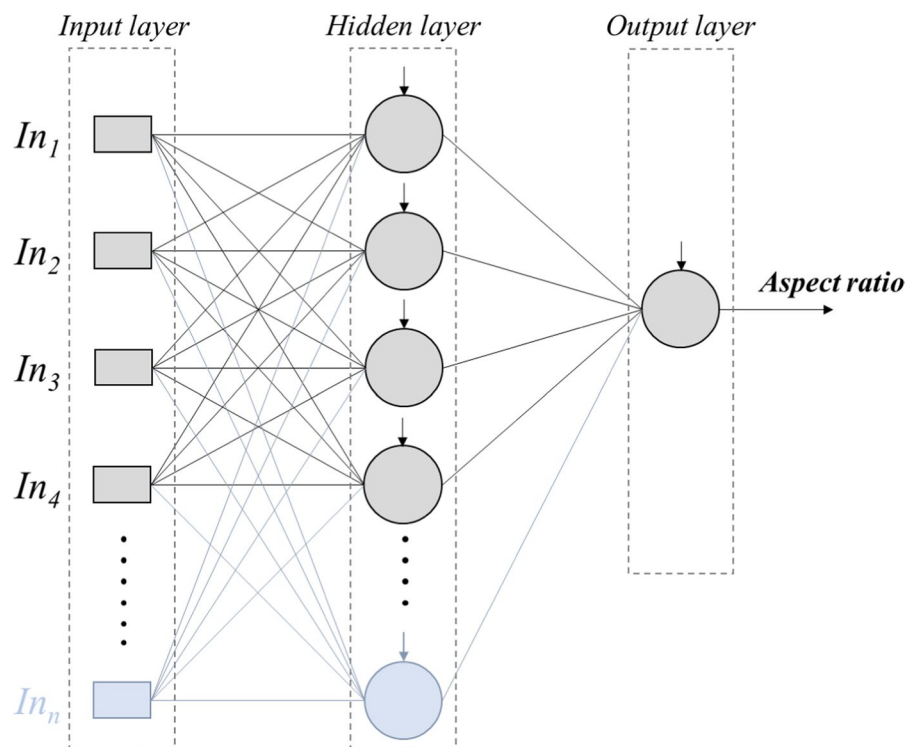


**Table 2** Ranges of the experimental data used for ANN modelling (published elsewhere and available in Tables S1 and S2)

Type of variable	Variable	Range	Units
Pulp characteristics (input)	Cellulose content	47.9–85.3	wt%
	Hemicellulose content	8.7–22.9	wt%
	Insoluble lignin content	0.5–15.8	wt%
	Soluble lignin content	3.4–11.2	wt%
	Length weighted in length	377–449	µm
	Diameter	20.7–29.3	µm
	Fines content	33.1–54.5	%
Process parameters (input)	Carboxyl content	53–66	µeq/g
	HPH—Energy consumption	5.67–19.72	kWh/kg
LCNF characteristics (input)	Consistency	0.89–0.98	wt%
	Cationic demand	148–210	µeq/g
	Transmittance at 600 nm	2.5–12.7	%
	Consistency index “K”	0.222–7.679	–
Output	Flow behavior index “n”	0.204–0.373	–
	Aspect ratio	51–217	–

The dataset included 15 samples based on pine pulps (TMP, UKSP and BKSP), which was normalized between 0.0 and 1.0 and randomly partitioned into 3 subsets, namely training, validation and testing data (70%, 15% and 15% of experimental data, respectively). The numerical verification of the performance of the networks was done by computing the mean square error (MSE), which is minimized during the network training process. According to Eq. 1, MSE considers the sample differences between predicted values ( $\hat{y}_j$ ) and observed ones ( $y_j$ ). Additionally, the correlation coefficient (R) was evaluated in accordance with Eq. 2, where  $\bar{y}$  stands for the arithmetic mean of experimental values of the output variable.

$$MSE = \frac{1}{N} \sum_{j=1}^n (y_j - \hat{y}_j)^2 \quad (1)$$

$$R = \sqrt{1 - \frac{\sum_{j=1}^n (y_j - \hat{y}_j)^2}{\sum_{j=1}^n (y_j - \bar{y})^2}} \quad (2)$$

The optimization of the ANN architecture was performed by minimizing the testing error, considering repeated neural network calculations involving different combinations of inputs (3–10) and number of neurons in the hidden layer (1–12).

Special attention was given towards reducing the ANN architecture's size, and consequently diminishing the number of weights, thus avoiding overfitting the calibration experimental data. To accomplish that, the level of significance of input variables was assessed by sensitivity analysis using the procedure proposed by Yoon et al. in accordance to Eq. 3 (Yoon et al. 1993). This equation measures the relative strength ( $RS_{ji}$ ) between the  $i$ th input and the  $j$ th output variables, where  $w_{ki}$  is the weight between the  $k$ th hidden neuron and the  $i$ th input, and  $w_{jk}$  is the weight between the  $j$ th output and the  $k$ th hidden neuron, considering an ANN model with  $n$  hidden neurons and  $m$  inputs. All the calculations were carried out in Matlab R2019a software.

$$RS_{ji}(\%) = \frac{\sum_{k=0}^n (w_{ki} - w_{jk})}{\sum_{i=0}^m \left| \sum_{k=0}^n (w_{ki} - w_{jk}) \right|} \times 100\% \quad (3)$$

## Results and discussion

### ANN input selection: pine pulps analysis

To discriminate the importance of each input variable on the aspect ratio of the micro-nanofibers, several ANNs were trained considering the architecture

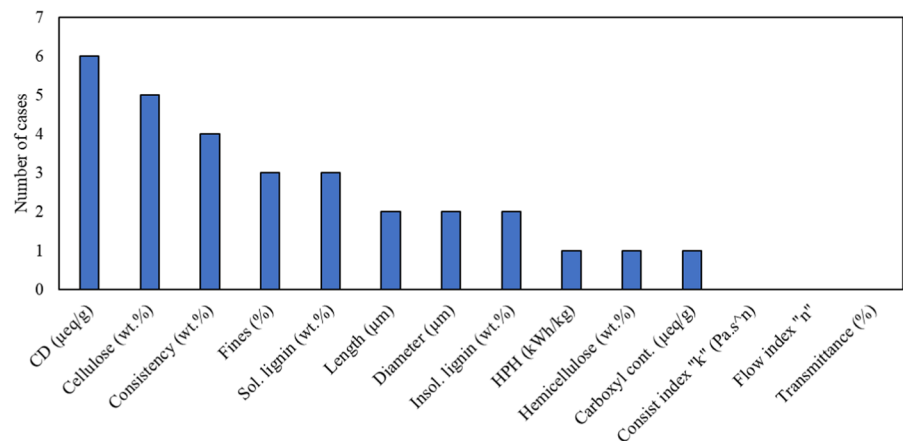
3-5-1 (i.e., 3 inputs, 5 neurons in the hidden layer and 1 output) for which all possible combinations of the 14 inputs were used on the basis of variables reported in Table 1. The dataset employed during these preliminary modeling tests was based on the characterization data of LCMNFs produced from pine pulps (TMP, UKSP and BKSP). The procedure yielded 364 ANN input combinations. All of them were calculated 1000 times and the one that provided the lowest MSE to the testing subset was selected for each combination. These 364 ANN models were ranked in terms of MSE and the top-10 ANN models were selected to assess the most frequent inputs, as summarized in Fig. 3. The evaluation of inputs revealed that there were 3 variables which never appeared as inputs for these top-10 models: rheological variables coming from the power law model (coefficients  $K$  and  $n$ ) and the optical transmittance at 600 nm. Checking when these variables would leave from zero and reach at least the unit in this graph, it would be necessary to plot the top-43 ( $K$ ), top-44 (transmittance) and top-49 ( $n$ ). From these results, it seems that, regardless of the well-recognized relationship between rheological parameters and the aspect ratio, there are several other variables that deserves priority when we want to describe the aspect ratio using a nonlinear approach (Moberg et al. 2017).

Another interesting remark from these results is the deep influence of the chemical composition of the LCMNFs upon the output variable. This is expected because the dataset involved samples with a wide interval of chemical composition patterns, which ultimately may contribute to explain the aspect ratio behavior. In addition, the HPH process

was based on constant application of energy, which provides a more relevant role to inherent characteristics, rather than process conditions. However, the influence of chemical composition on the resulting LCMNF characteristics has been previously highlighted by several authors, particularly the effect of residual lignin and hemicellulose (Syverud et al. 2011; Ferrer et al. 2012; Delgado-Aguilar et al. 2016; Tarrés et al. 2017b). For this same reason, the cationic demand (CD), in the range of 148–210  $\mu\text{eq/g}$  for pine pulps) appears as the most frequent input on the top-10 ANN models. Indeed, the best 6 ANN models on this list included CD as input, which clearly shows the importance of this variable. Experimental evidence from our previous work demonstrated that CD was mainly dependent on the HPH intensity and well correlated to the rheological parameter  $K$  (Serra-Parareda et al. 2021b). In addition, the CD has been also reported to have a direct influence on the SSA of fibers and fines, which may also influence the aspect ratio of the resulting LCMNFs (Serra-Parareda et al. 2021a).

These results support the idea that the HPH intensity, represented by the applied energy, and  $K$  lose their relevance on the description of the aspect ratio if the CD is employed as input in the ANN model. However, this does not mean that these former variables should be discarded from the investigation, because here we restricted ourselves to the specific case of 3-5-1 ANN modeling architecture, which means that they could be important for other architecture training. Indeed, the CD has been reported to be strongly correlated with fibrillation energy regardless the fibrillation equipment (Tarrés et al. 2020).

**Fig. 3** The most frequent ANN inputs considering a 3-5-1 architecture: top-ten ANN models



Based on the previous results, the relative strength (RS) of the different inputs on the predicted aspect ratio was evaluated. ANNs were calculated repeatedly considering many inputs (8) and 10 neurons in the hidden layer. For these calculations, certain variables were removed from the dataset (transmittance,  $K$ ,  $n$  and carboxyl content) since preliminary tests indicated no significant influence on ANN modeling. CD was also excluded from the dataset, as the preliminary tests revealed that this variable hampered the contribution of HPH on the aspect ratio models. This was completely expected, as the aspect ratio determination may be influenced by the surface charge of the LCMNFs due to the selected methodology for its determination, namely gel point (Sanchez-Salvador et al. 2021b). Figure 4 summarizes the mean relative strength of the inputs upon the aspect ratio predicted by ANN models with 8-10-1 architecture. Note that there are 3 inputs linked to the chemical composition with negligible impact on the ANN output: hemicellulose (2.9%), insoluble lignin (−1.8%) and soluble lignin (0.2%). Also, the impact of the fines contents was negative. On the other hand, concerning the most relevant inputs which positively influenced the aspect ratio, in order of importance, Length, HPH, Diameter and Cellulose content were identified.

From the previous sensitivity analysis, additional ANN modeling was performed considering the reduction of the input variables to the 4 inputs outlined above, and different amounts of hidden neurons. The performance of these ANN models trained with pine

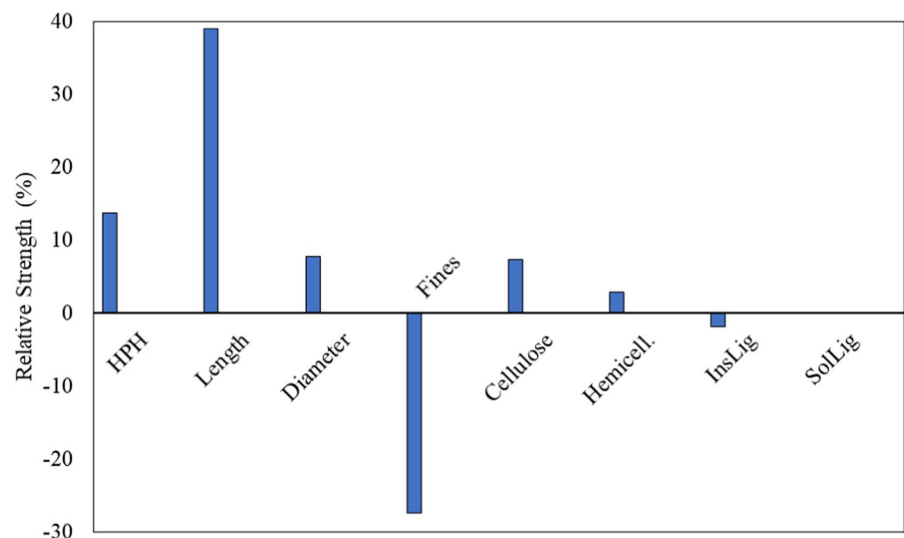
dataset for training (75% of the whole dataset), validation (15% of the dataset) and testing (15% remaining) is summarized in Table 3, considering ANN architectures with 4 or 3 inputs (by removing the Diameter in the input layer). It can be verified that the ANN models provide very good experimental data fitting for all architectures, yielding high correlation coefficient ( $R > 0.99$ ) for either the training or the validation subset. Concerning the 4-input ANN models, the reduction of the number of hidden neurons from 6 to 3 improved all the performance parameters, leading to enhanced  $R$  (training, validation, and testing subsets) and reduced MSE. Further hidden neuron reduction seems to be not advantageous for the

**Table 3** ANN models performance with HPH, Length, Diameter and Cellulose content

ANN architecture	Correlation coefficient (R)			
	Training	Validation	Testing	MSE
4-6-1	0.9981	0.9918	0.9876	4.14E-03
4-4-1	0.9993	0.9989	0.9984	5.43E-04
4-3-1	0.9997	0.9995	0.9988	2.42E-05
4-2-1	0.9979	0.9991	0.9986	4.72E-04
4-1-1	0.9920	0.9946	0.9887	2.72E-03
3-3-1 <sup>a</sup>	0.9993	0.9992	0.9989	7.42E-05
3-2-1 <sup>a</sup>	0.9955	0.9985	0.9978	7.43E-04
3-1-1 <sup>a</sup>	0.9917	0.9973	0.9895	1.36E-03

<sup>a</sup>Tests performed excluding the variable Diameter in the input layer

**Fig. 4** RS of the selected input variables over output variable according to Yoon et al. for ANN models considering 8-10-1 architecture (Yoon et al. 1993)





system under investigation, because it compromises the MSE and R-testing performance. In fact, from these results, it can be concluded that the optimum number of neurons in the hidden layer is 3, since it provided the best ANN model performance in tests involving both 4 and 3 inputs. Finally, Fig. 5 shows a very good agreement between experimental data and ANN model predictions (normalized data) during the neural networks training, indicating that the ANN models calculated here are good enough to capture the nonlinearities behind the dataset for the prediction of the aspect ratio, also revealing the high quality of models involving solely 3 hidden neurons.

The fibrillation intensity has been reported to directly influence the morphology of micro- and nanostructured cellulose. Indeed, increasing HPH intensity usually leads to higher surface area, which indicates significant changes on morphology, but also on a significant reduction of fiber length (Ang et al. 2019). However, the applied energy to lignocellulosic fibers influence the resulting characteristics of LCMNFs in different ways, depending on other aspects such as chemical composition, initial fiber length, and the presence of functional groups at fiber surface (i.e. carboxyl groups in TEMPO-mediated oxidation)

(Rodionova et al. 2013; Rojo et al. 2015; Filipova et al. 2018; Serra-Parareda et al. 2021d). In fact, this was already observed by Turbak et al. (1983) in their renowned study on properties, uses and commercial potential of microfibrillated cellulose, where the authors already reported the need of adjusting the fibril length prior to fibrillation (Turbak et al. 1983). In a more recent review, the effect of hyper inertial flows over the properties of micro- and nanostructured cellulose has been studied, indicating that fibril morphology may be altered by means of modifying flow patterns. Indeed, authors identified that hyper inertial flow, occurring in microfluidizers and high-pressure homogenizers, had different effect on long and short fibers, clearly indicating that fiber length directly influences the morphological changes that fibrils experience (Redlinger-Pohn et al. 2022).

#### ANN model validation with other fiber sources

The developed ANN models were validated with additional LCMNFs, which did not take part of the modelling, training, testing and first validation processes. Concretely, LCMNFs from Spruce BTMP (Serra-Parareda et al. 2021b), Eucalyptus BKHP

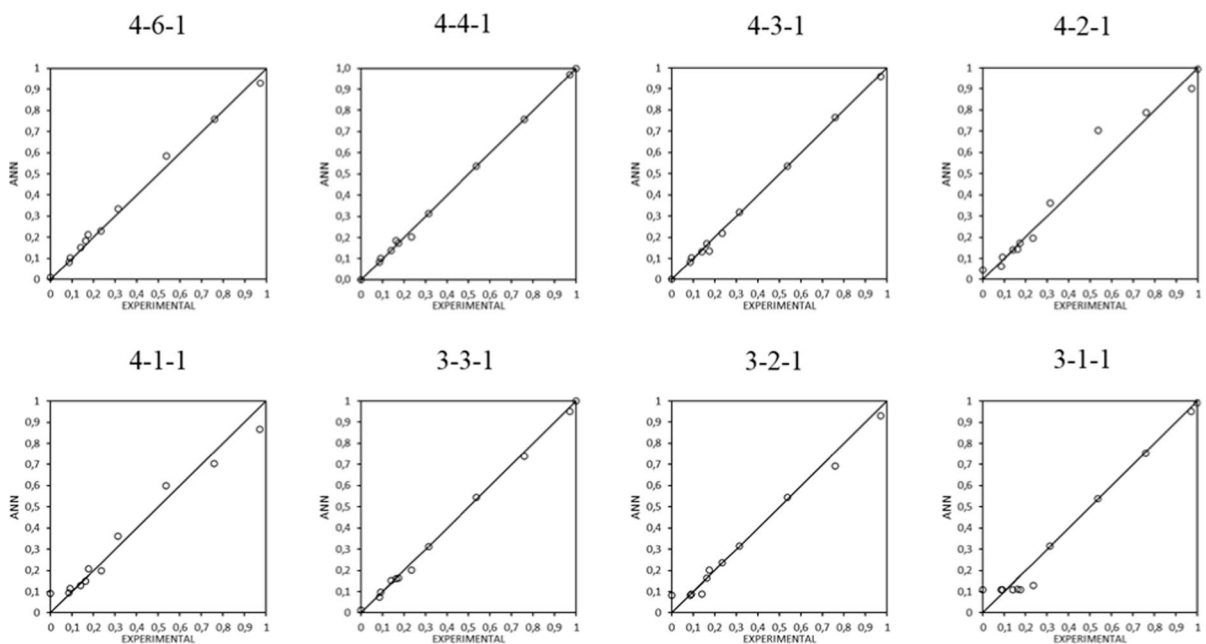


**Fig. 5** Comparison between experimental and ANN predictions of aspect ratio using different ANN model architectures (see Table 3)

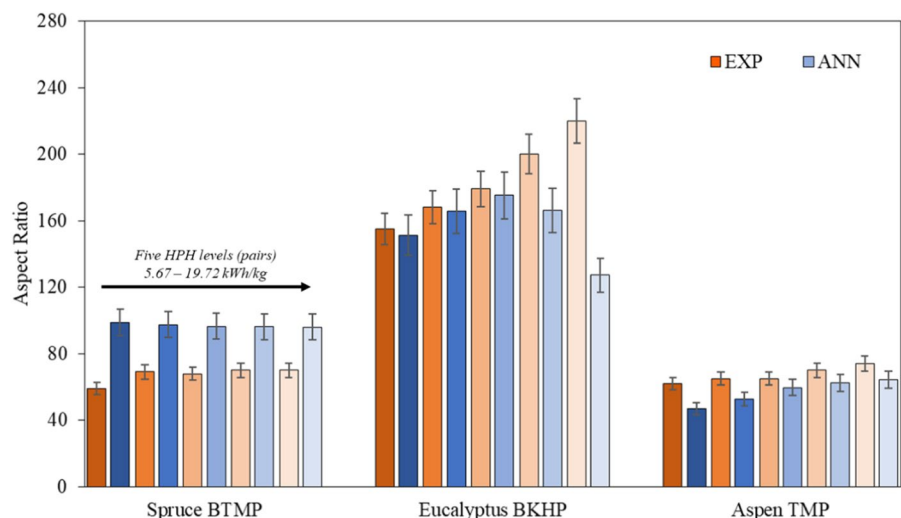
(Sanchez-Salvador et al. 2021a) and Aspen TMP (Balea et al. 2021b) were used, as reported in Tables S1 and S2 from the Supplementary Material.

Figure 6 shows the predictions of aspect ratio compared to the experimental values after applying an ANN architecture of 4-4-1. Although not exhibiting the best performance among the models summarized in Table 3, this architecture was selected due to its versatility and good performance to the selected LCMNFs, yielding a suited correlation ( $R=0.84$ ) regardless the fiber source. The values reported in Fig. 6 were organized in five levels of HPH intensity, represented in pairs from left to right. As it can be clearly seen, a good agreement between ANN model predictions and experimental data occurred for the Aspen TMP LCMNFs. Despite the offset between predictions and experimental data for Aspen TMP, the model could follow the slight increase of the aspect ratio with the homogenization. Recall that the ANN models trained here were based exclusively on Pine patterns, which could increase the risk of model failing when subjected to data from very different materials. Proper predictions were provided by the ANN model for Eucalyptus BKHP. As shown in the graph, although some loss of accuracy did occur for some of these samples, the model was able to follow extremely well the experimental values of aspect ratio for the first 3 HPH levels. Indeed, similarly to the case of model predictions for Aspen TMP, the neural network seemed to capture the dynamics of increase of the aspect ratio with the severity of the HPH. This behavior of Eucalyptus BKHP was observed before

and attributed to a fibrillation effect linked to the decrease in the diameter of the original fibers due to peeling (Sanchez-Salvador et al. 2021a). Moreover, the ANN model provided satisfactory predictions of aspect ratio for Spruce BTMP. For these fibers, even though the model overestimated the aspect ratio, predictions indicated no increase of this characteristic with further homogenization, likewise in the Spruce BTMP experimental data. These results show that there is a set of features that govern the aspect ratio of LCMNFs produced from different wood sources, and that empirical neural network models can be built to correlate them fairly well.

Spruce BTMP, coming from softwood, exhibited a similar behavior to the Pine pulps selected for modelling, testing, and training of the developed ANNs. This indicates that the developed ANN models based on Pine data could be useful for other softwood species. This might be expectable, as thermomechanical pulps from softwood species were included in the model, and it exhibits similar cellulose, hemicellulose, and lignin content to Pine TMP. However, fiber length was significantly different, and because this feature has shown the highest relative strength out of all the selected input variables (as seen in Fig. 4), this may explain the overestimation of the aspect ratio of the model compared to experimental values. Apparently, the developed ANN with the 4-4-1 architecture provides excellent estimations with thermomechanical pulps, as Aspen TMP exhibited the lowest differences between experimental and predicted values. This may be explained by the similarities in both

**Fig. 6** Independent validation results of aspect ratio predicted by ANN model 4-4-1 at different (and increasing) HPH levels



chemical composition and morphology of Aspen TMP, Spruce BTMP and Pine TMP, although the first is a hardwood specie. The most significant difference between those LCMNFs obtained from Aspen TMP and the rest was found in the transmittance at 600 nm (except for Eucalyptus BKHP, which does not contain lignin and this measurement may be hampered), indicating that the higher presence of lignin promoted fibrillation and increase on surface area rather than effects on aspect ratio (Rojo et al. 2015). Finally, Eucalyptus BKHP, another hardwood specie, also led to LCMNFs whose characteristics fitted the predictive model, particularly at low HPH intensity. This may be explained by the differences between eucalyptus and pine. BKHP has been reported to be less crystalline than BKSP, which may limit the fiber fragmentation during fibrillation and, thus, leading to longer fibers. As the ANN models were prepared with softwood species, this might not be considered and, thus, at higher HPH intensity, higher error (Syverud et al. 2011; Tarrés et al. 2019).

## Conclusions

The use of ANN to model the morphological features of the micro-nanocellulose segment is still an original area of study. One difficulty with this approach is the need for a large amount of experimental data to fit the model. In this work, ANNs were trained to predict the aspect ratio of (ligno)cellulose micro/nanofibers. The calibration dataset was constructed using only data from Pine pulps described in earlier works including just 15 samples that had undergone thermo-mechanical, kraft and bleached kraft treatments. The selection of input variables of the fibrillation process was carried out thoroughly, combining with the interpretation of the behavior of the actual process conditions, allowing to identify that the aspect ratio could be properly described by four main inputs: cellulose contents, applied energy, the mean fiber length and the mean diameter of the pre-treated pulps. The neural model based on these 4 inputs and on 4 neurons in the hidden layer showed excellent correlation with the dataset used in the calibration ( $R=0.9993$ ), validation ( $R=0.9989$ ) and testing ( $R=0.9984$ ) stages. In addition, the neural model showed good ability to predict the aspect ratio of nanofiber materials obtained from different cellulose sources ( $R=0.84$ )

including softwood pulp from Spruce BTMP, and (to a greater extent) hardwood pulps from Eucalyptus BKHP and Aspen TMP. Besides, the model was able to provide interesting insight into the evolution of the aspect ratio with the progressive increase of the energy applied throughout the fibrillation process. These results are encouraging and show that the neural network modeling strategy presented here is quite useful to predict the aspect ratio of (ligno)cellulose micro/nanofibers on the basis of a set of easy-to-measure operation variables and initial fiber characteristics, which makes this technique very attractive from an industrial perspective in order to control de product quality.

**Acknowledgments** This work was carried out as a part of the UFPR-Capes-PrInt cooperation project with University of Girona, Spain. The authors wish to acknowledge the financial support of the Spanish Ministry of Science and Innovation to the project CON-FUTURO-ES (PID2020-113850RB-C21 and PID2020-113850RB-C22) and VALORCON-NC (PDC2021-120964-C21 and PDC2021-120964-C22). Alexandre F. Santos acknowledges CNPq (Conselho Nacional de Desenvolvimento Científico e Tecnológico) for supporting this work. Marc Delgado-Aguilar is a Serra Hünter Fellow.

**Funding** Open Access funding provided thanks to the CRUE-CSIC agreement with Springer Nature.

## Declarations

**Conflict of interest** Authors declare that they have no known competing interests or personal relationships that could have appeared to influence the work reported in this paper.

**Open Access** This article is licensed under a Creative Commons Attribution 4.0 International License, which permits use, sharing, adaptation, distribution and reproduction in any medium or format, as long as you give appropriate credit to the original author(s) and the source, provide a link to the Creative Commons licence, and indicate if changes were made. The images or other third party material in this article are included in the article's Creative Commons licence, unless indicated otherwise in a credit line to the material. If material is not included in the article's Creative Commons licence and your intended use is not permitted by statutory regulation or exceeds the permitted use, you will need to obtain permission directly from the copyright holder. To view a copy of this licence, visit <http://creativecommons.org/licenses/by/4.0/>.

## References

- Almonti D, Baiocco G, Tagliaferri V, Ucciardello N (2019) Artificial neural network in fibres length prediction for

- high precision control of cellulose refining. *Materials* (Basel) 12:3730. <https://doi.org/10.3390/ma12223730>
- Ang S, Haritos V, Batchelor W (2019) Effect of refining and homogenization on nanocellulose fiber development, sheet strength and energy consumption. *Cellulose* 26:4767–4786. <https://doi.org/10.1007/s10570-019-02400-5>
- Balea A, Blanco A, Delgado-Aguilar M et al (2021a) Nanocellulose characterization challenges. *BioResources* 16:4382–4410
- Balea A, Fuente E, Tarrés Q et al (2021b) Influence of pretreatment and mechanical nanofibrillation energy on properties of nanofibers from aspen cellulose. *Cellulose* 28:9187–9206. <https://doi.org/10.1007/s10570-021-04109-w>
- Boufi S, González I, Delgado-Aguilar M et al (2016) Nanofibrillated cellulose as an additive in papermaking process: a review. *Carbohydr Polym*. <https://doi.org/10.1016/j.carbpol.2016.07.117>
- De France KJ, Hoare T, Cranston ED (2017) Review of hydrogels and aerogels containing nanocellulose. *Chem Mater* 29:4609–4631. <https://doi.org/10.1021/acs.chemmater.7b00531>
- Delgado-Aguilar M, González I, Tarrés Q et al (2016) The key role of lignin in the production of low-cost lignocellulosic nanofibres for papermaking applications. *Ind Crops Prod* 86:295–300. <https://doi.org/10.1016/j.indcrop.2016.04.010>
- Desmaisons J, Boutonnet E, Rueff M et al (2017) A new quality index for benchmarking of different cellulose nanofibrils. *Carbohydr Polym* 174:318–329. <https://doi.org/10.1016/j.carbpol.2017.06.032>
- Dimic-Misic K, Maloney T, Gane P (2018) Effect of fibril length, aspect ratio and surface charge on ultralow shear-induced structuring in micro and nanofibrillated cellulose aqueous suspensions. *Cellulose* 25:117–136. <https://doi.org/10.1007/s10570-017-1584-3>
- Espinosa E, Tarrés Q, Delgado-Aguilar M et al (2016) Suitability of wheat straw semichemical pulp for the fabrication of lignocellulosic nanofibres and their application to papermaking slurries. *Cellulose*. <https://doi.org/10.1007/s10570-015-0807-8>
- Ferrer A, Quintana E, Filpponen I et al (2012) Effect of residual lignin and heteropolysaccharides in nanofibrillar cellulose and nanopaper from wood fibers. *Cellulose*. <https://doi.org/10.1007/s10570-012-9788-z>
- Filipova I, Fridrihsone V, Cabulis U, Berzins A (2018) Synthesis of nanofibrillated cellulose by combined ammonium persulphate treatment with ultrasound and mechanical processing. *Nanomaterials*. <https://doi.org/10.3390/nano8090640>
- Filipova I, Serra F, Tarrés Q et al (2020) Oxidative treatments for cellulose nanofibers production: a comparative study between TEMPO-mediated and ammonium persulfate oxidation. *Cellulose*. <https://doi.org/10.1007/s10570-020-03089-7>
- Foster EJ, Moon RJ, Agarwal UP et al (2018) Current characterization methods for cellulose nanomaterials. *Chem Soc Rev* 47:2609–2679. <https://doi.org/10.1039/c6cs00895j>
- Future Markets Inc. (2020) The global market for cellulose nanofibers. <https://www.futuremarketsinc.com/the-global-market-for-cellulose-nanofibers/>
- Gu F, Wang W, Cai Z et al (2018) Water retention value for characterizing fibrillation degree of cellulosic fibers at micro and nanometer scales. *Cellulose* 25:2861–2871. <https://doi.org/10.1007/s10570-018-1765-8>
- Henriksson M, Henriksson G, Berglund LA, Lindström T (2007) An environmentally friendly method for enzyme-assisted preparation of microfibrillated cellulose (MFC) nanofibers. *Eur Polym J* 43:3434–3441. <https://doi.org/10.1016/j.eurpolymj.2007.05.038>
- Himmelblau DM (2000) Applications of artificial neural networks in chemical engineering. *Korean J Chem Eng* 17:373–392
- Hubbe MA, Tayeb P, Joyce M et al (2017) Rheology of nanocellulose-rich aqueous suspensions: a review. *BioResources* 12:9556–9661. <https://doi.org/10.15376/biores.12.4.Hubbe>
- Isogai A (2020) Emerging nanocellulose technologies: recent developments. *Adv Mater*. <https://doi.org/10.1002/adma.202000630>
- Iwamoto S, Lee S-H, Endo T (2014) Relationship between aspect ratio and suspension viscosity of wood cellulose nanofibers. *Polym J* 46:73–76. <https://doi.org/10.1038/pj.2013.64>
- Jonoobi M, Oladi R, Davoudpour Y et al (2015) Different preparation methods and properties of nanostructured cellulose from various natural resources and residues: a review. *Cellulose* 22:935–969. <https://doi.org/10.1007/s10570-015-0551-0>
- Kangas H, Lahtinen P, Sneek A et al (2014) Characterization of fibrillated celluloses. A short review and evaluation of characteristics with a combination of methods. *Nord Pulp Pap Res J* 29:129–143
- Kim JH, Shim BS, Kim HS et al (2015) Review of nanocellulose for sustainable future materials. *Int J Precis Eng Manuf: Green Technol* 2:197–213
- Klemm D, Cranston ED, Fischer D et al (2018) Nanocellulose as a natural source for groundbreaking applications in materials science: today's state. *Mater Today* 21:720–748. <https://doi.org/10.1016/j.mattod.2018.02.001>
- Kubat M (1999) Neural networks: a comprehensive foundation by Simon Haykin, Macmillan, 1994, 409–412, ISBN 0-02-352781-7. *Knowl Eng Rev* 13(4):409–412
- Kumar V, Pathak P, Bhardwaj NK (2020) Waste paper: an underutilized but promising source for nanocellulose mining. *Waste Manag* 102:281–303
- Li MC, Wu Q, Moon RJ et al (2021a) Rheological aspects of cellulose nanomaterials: governing factors and emerging applications. *Adv Mater* 33:2006052
- Li T, Chen C, Brozena AH et al (2021b) Developing fibrillated cellulose as a sustainable technological material. *Nature* 590:47–56. <https://doi.org/10.1038/s41586-020-03167-7>
- Moberg T, Sahlin K, Yao K et al (2017) Rheological properties of nanocellulose suspensions: effects of fibril/particle dimensions and surface characteristics. *Cellulose* 24:2499–2510. <https://doi.org/10.1007/s10570-017-1283-0>
- Nguyen D, Widrow B (1990) Improving the learning speed of 2-layer neural networks by choosing initial values of the adaptive weights. In: 1990 IJCNN international joint conference on neural networks. vol. 3, pp 21–26

- Oksman K, Aitomäki Y, Mathew AP et al (2016) Review of the recent developments in cellulose nanocomposite processing. *Compos Part A Appl Sci Manuf* 83:2–18. <https://doi.org/10.1016/j.compositesa.2015.10.041>
- Osong SH, Norgren S, Engstrand P (2013) An approach to produce nano-ligno-cellulose from mechanical pulp fine materials. *Nord Pulp Pap Res J* 28:472–479. <https://doi.org/10.3183/npprj-2013-28-04-p472-479>
- Qua EH, Hornsby PR, Sharma HSS, Lyons G (2011) Preparation and characterisation of cellulose nanofibres. *J Mater Sci* 46:6029–6045. <https://doi.org/10.1007/s10853-011-5565-x>
- Redlinger-Pohn JD, Brouzet C, Aulin C et al (2022) Mechanisms of cellulose fiber comminution to nanocellulose by hyper inertia flows. *ACS Sustain Chem Eng* 10:703–719. <https://doi.org/10.1021/acssuschemeng.1c03474>
- Rodionova G, Saito T, Lenés M et al (2013) TEMPO-mediated oxidation of norway spruce and eucalyptus pulps: preparation and characterization of nanofibers and nanofiber dispersions. *J Polym Environ* 21:207–214. <https://doi.org/10.1007/s10924-012-0483-9>
- Royo E, Peresin MS, Sampson WW et al (2015) Comprehensive elucidation of the effect of residual lignin on the physical, barrier, mechanical and surface properties of nanocellulose films. *Green Chem* 17:1853–1866. <https://doi.org/10.1039/c4gc02398f>
- Saito T, Kimura S, Nishiyama Y, Isogai A (2007) Cellulose nanofibers prepared by TEMPO-mediated oxidation of native cellulose. *Biomacromol* 8:2485–2491. <https://doi.org/10.1021/bm0703970>
- Sanchez-Salvador JL, Monte MC, Batchelor W et al (2020) Characterizing highly fibrillated nanocellulose by modifying the gel point methodology. *Carbohydr Polym* 227:115340. <https://doi.org/10.1016/j.carbpol.2019.115340>
- Sanchez-Salvador JL, Campano C, Lopez-Exposito P et al (2021a) Enhanced morphological characterization of cellulose nano/microfibers through image skeleton analysis. *Nanomaterials* 11:2077. <https://doi.org/10.3390/nano11082077>
- Sanchez-Salvador JL, Monte MC, Negro C et al (2021b) Simplification of gel point characterization of cellulose nano and microfiber suspensions. *Cellulose* 28:6995–7006. <https://doi.org/10.1007/s10570-021-04003-5>
- Sanchez-Salvador JL, Campano C, Balea A et al (2022) Critical comparison of the properties of cellulose nanofibers produced from softwood and hardwood through enzymatic, chemical and mechanical processes. *Int J Biol Macromol* 205:220–230. <https://doi.org/10.1016/j.ijbiomac.2022.02.074>
- Serra-Parareda F, Aguado R, Tarrés Q et al (2021a) Chemical-free production of lignocellulosic micro- and nanofibers from high-yield pulps: synergies, performance, and feasibility. *J Clean Prod* 313:1–10. <https://doi.org/10.1016/j.jclepro.2021.127914>
- Serra-Parareda F, Tarrés Q, Mutjé P et al (2021b) Correlation between rheological measurements and morphological features of lignocellulosic micro/nanofibers from different softwood sources. *Int J Biol Macromol* 187:789–799. <https://doi.org/10.1016/j.ijbiomac.2021.07.195>
- Serra-Parareda F, Tarrés Q, Pèlach MÀ et al (2021c) Monitoring fibrillation in the mechanical production of lignocellulosic micro/nano fibers from bleached spruce thermomechanical pulp. *Int J Biol Macromol* 178:354–362. <https://doi.org/10.1016/j.ijbiomac.2021.02.187>
- Serra-Parareda F, Tarrés Q, Sanchez-Salvador JL et al (2021d) Tuning morphology and structure of non-woody nanocellulose: Ranging between nanofibers and nanocrystals. *Ind Crops Prod* 171:113877. <https://doi.org/10.1016/j.indcrop.2021.113877>
- Solala I, Volperts A, Andersone A et al (2012) Mechanoradical formation and its effects on birch kraft pulp during the preparation of nanofibrillated cellulose with Masuko refining. *Holzforchung* 66:477–483. <https://doi.org/10.1515/HF.2011.183>
- Syverud K, Chinga-Carrasco G, Toledo J, Toledo PG (2011) A comparative study of eucalyptus and pinus radiata pulp fibres as raw materials for production of cellulose nanofibrils. *Carbohydr Polym* 84:1033–1038. <https://doi.org/10.1016/j.carbpol.2010.12.066>
- Taheri H, Samyn P (2016) Effect of homogenization (microfluidization) process parameters in mechanical production of micro- and nanofibrillated cellulose on its rheological and morphological properties. *Cellulose* 23:1221–1238. <https://doi.org/10.1007/s10570-016-0866-5>
- Tanaka R, Saito T, Ishii D, Isogai A (2014) Determination of nanocellulose fibril length by shear viscosity measurement. *Cellulose* 21:1581–1589. <https://doi.org/10.1007/s10570-014-0196-4>
- Tanaka R, Saito T, Hondo H, Isogai A (2015) Influence of flexibility and dimensions of nanocelluloses on the flow properties of their aqueous dispersions. *Biomacromol* 16:2127–2131. <https://doi.org/10.1021/acs.biomac.5b00539>
- Tarrés Q, Boufi S, Mutjé P, Delgado-Aguilar M (2017a) Enzymatically hydrolyzed and TEMPO-oxidized cellulose nanofibers for the production of nanopapers: morphological, optical, thermal and mechanical properties. *Cellulose* 24:3943–3954. <https://doi.org/10.1007/s10570-017-1394-7>
- Tarrés Q, Ehman NVNVN, Vallejos MEME et al (2017b) Lignocellulosic nanofibers from triticale straw: the influence of hemicelluloses and lignin in their production and properties. *Carbohydr Polym* 163:20–27. <https://doi.org/10.1016/j.carbpol.2017.01.017>
- Tarrés Q, Mutjé P, Delgado-Aguilar M (2019) Towards the development of highly transparent, flexible and water-resistant bio-based nanopapers: tailoring physico-mechanical properties. *Cellulose* 26:6917–6932. <https://doi.org/10.1007/s10570-019-02524-8>
- Tarrés Q, Oliver-Ortega H, Boufi S et al (2020) Evaluation of the fibrillation method on lignocellulosic nanofibers production from eucalyptus sawdust: a comparative study between high-pressure homogenization and grinding. *Int J Biol Macromol* 145:1199–1207. <https://doi.org/10.1016/j.IJBIO MAC.2019.10.046>
- Torrents-Barrena J, Pellicer E (2021) Smart cellulose composites: advanced applications and properties prediction using machine learning. *Encycl Mater: Compos* 2:527–538. <https://doi.org/10.1016/B978-0-12-819724-0.00058-6>
- Turbak AF, Snyder FW, Sandberg KR (1983) Microfibrillated cellulose, a new cellulose product: properties, uses, and commercial potential. *J Appl Polym Sci Appl Polym Symp* 37(9):815–827

- Wu Q, Meng Y, Wang S et al (2014) Rheological behavior of cellulose nanocrystal suspension: influence of concentration and aspect ratio. *J Appl Polym Sci* 131:1–8. <https://doi.org/10.1002/app.40525>
- Wu Q, Li X, Fu S et al (2017) Estimation of aspect ratio of cellulose nanocrystals by viscosity measurement: influence of surface charge density and NaCl concentration. *Cellulose* 24:3255–3264. <https://doi.org/10.1007/s10570-017-1341-7>
- Wu Q, Li X, Li Q et al (2019) Estimation of aspect ratio of cellulose nanocrystals by viscosity measurement: influence of aspect ratio distribution and ionic strength. *Polymers (Basel)* 11:1–12. <https://doi.org/10.3390/polym11050781>
- Yoon Y, Swales G, Margavio TM (1993) A comparison of discriminant analysis versus artificial neural networks. *J Oper Res Soc* 44:51–60. <https://doi.org/10.2307/2584434>

**Publisher's Note** Springer Nature remains neutral with regard to jurisdictional claims in published maps and institutional affiliations.